Assessment of Harir Basin Against Soil Erosion in Kurdistan Region-Iraq

Mustafa J. Saber ⓘ*, Jehan M. Sheikh Suleimany ⓘ

Department of Water Resources Engineering, College of Engineering, Salahaddin University, Erbil, Kurdistan Region, Iraq.

Highlights:

- The (USLE) has been integrated with (RS) and (GIS) techniques to create the spatial distribution of the annual rate of soil erosion.
- The spatial distribution of the (Average (R-Factor)), (K-Factor), (LS-Factor), (C-Factor), and (P-Factor) have been created using ArcGIS 10.8.1 software.
- The Supervised Classification-Maximum Likelihood Classification (MLC) has been used to classify the land use and land cover for Harir Basin using the ERDAS Imagine 2014 software based on Landsat 9 OLI images.
- The overall accuracy, producer accuracy, user accuracy, and Kappa coefficient have been calculated for the land use and land cover classification map.

*Corresponding author:

Mustafa J. Saber

Department of Water Resources Engineering, College of Engineering, Salahaddin University, Erbil, Kurdistan Region, Iraq.

Abstract: Soil erosion negatively impacts water management, agricultural lands, amounts of sedimentation in reservoirs and rivers, water pollution, human health, countries' economies, and ecosystems. This study is important for water, soil, and environment management. In the present study, the Universal Soil Loss Equation (USLE) has been integrated with the Remote Sensing (RS) and Geographic Information System (GIS) techniques to calculate the annual rate of soil erosion of Harir Basin and to classify it on this basis and according to the soil erosion risk classes. The spatial distribution of the average rainfall erosivity factor (Average (R-Factor)), soil erodibility factor (K-Factor), slope length and slope steepness factor (LS-Factor), cropping management factor (C-Factor), and conservation practice factor (P-Factor) have been created and mapped using ArcGIS 10.8.1 software based on the average annual rainfall map from (2000 to 2021), soil map, slope map in percentage with flow accumulation map, land use and land cover map, and slope map in percentage for Harir Basin, respectively. Overall, the results of assessing Harir Basin against soil erosion have illustrated that the annual rate of soil erosion for the area of study ranges from 0.0 $(\text{ton. ha}^{-1}.\text{year}^{-1})$ to 8.46 $(\text{ton. ha}^{-1}.\text{year}^{-1})$. Moreover, 99.99% of the study area was under slight soil erosion, while only 0.01% was under moderate soil erosion.

تقييم حوض حرير ضد انجراف التربة في إقليم كردستان-العراق

مصطفى جمعه صابر، جيهان محمد شيخ سليماني

قسم هندسة الموارد المائية / كلية الهندسة / جامعة صلاح الدين/ أربيل /إقليم كردستان – العراق.

الخلاصة

يؤثر انجراف التربة سلباً على إدارة المياه والأراضي الزراعية وكميات الترسبات في الخزانات والأنهار وتلوث المياه وصحة الإنسان واقتصادات البلدان والنظم البيئية. هذه الدراسة مهمة لإدارة المياه والتربة والبيئة. في هذه الدراسة، تم دمج المعادلة العالمية لفقدان التربة (USLE) مع تقنيات التحسس النائي (RS) ونظم المعلومات الجغرافية (GIS) لحساب المعدل السنوي لانجراف التربة في حوض حرير وتصنيفه على هذا الاساس ووفقًا لفئات مخاطر انجراف التربة. تم إنشاء ورسم التوزيع المكاني لمتوسط عامل الانجراف المطري ((R-Factor) (Average) وعامل انجراف التربة (K-Factor) و عامل طول المنحدر وانحدار المنحدر (LS-Factor) وعامل إدارة المحاصيل (C-Factor) و عامل ممارسة الحفظ (P-Factor) باستخدام برنامج ArcGIS 10.8.1 بناءً على خريطة متوسط هطول الأمطار السنوية من (٢٠٠٠ إلى ٢٠٢١) و خريطة التربة و خريطة المنحدر بالنسبة المئوية مع خريطة تراكم التدفق وخريطة استخدام الأراضي والغطاء الأرضي و خريطة المنحدر بالنسبة المئوية لحوض حرير، على التوالي. بشكل عام، أوضحت نتائج تقييم حوض حرير ضد انجراف التربة أن المعدل السنوي لانجراف التربة لمنطقة الدراسة يتراوح بين ٠,٠ ($\text{ton.ha}^{-1}.\text{year}^{-1}$) إلى ٨,٤٦ ($\text{ton.ha}^{-1}.\text{year}^{-1}$). علاوة على ذلك، ٩٩,٩٩٪ من منطقة الدراسة كانت تحت انجراف التربة الطفيفة، بينما ٠,٠١٪ فقط كانت تحت انجراف التربة المعتدلة.

الكلمات الدالة: متوسط عامل الانجراف المطري ((R-Factor) (Average)، عامل ممارسة الحفظ (P-Factor)، عامل إدارة المحاصيل (C-Factor)، حوض حرير، عامل طول المنحدر وانحدار المنحدر (LS-Factor)، عامل انجراف التربة (K-Factor)، المعادلة العالمية لفقدان التربة (USLE).

1.INTRODUCTION

During the 20th century, soil erosion has been widely increased worldwide as it has become a global issue of great social and environmental concern [1]. Water and wind are considered the main reasons for soil erosion, while water has been proven to be the main cause globally [2]. Lal [3] reported that 1094.0 million (ha) and 548.0 million (ha) are affected by soil erosion worldwide due to water and wind, respectively. Soil erosion increases sedimentation, increasing the proportion of phosphorus and nitrogen and producing eutrophication in the water bodies [4, 5], decreasing the streams and retention ponds capacity, reducing the intended life of the water resources facilities, and increasing the likelihood of flooding [6, 7]. Moreover, soil erosion negatively impacts soil productivity [8, 9] by increasing the salinity rate in the area due to the deterioration and inefficiency of the drainage systems in agricultural watersheds [10]. Soil erosion could be more dangerous and severe in the future due to the noticeable climatic changes in many regions worldwide [11]. In Asia, the average rate of soil erosion was 138.0 $(\text{ton.ha}^{-1}.\text{year}^{-1})$ [12], while Barrow [13] reported that the average soil erosion rate in South America, Africa, and Asia ranged from 30.0 to 40.0 $(\text{ton.ha}^{-1}.\text{year}^{-1})$. In Morocco, El Jazouli et al. [14] found that the total annual potential soil loss was about 70.660 $(\text{ton.ha}^{-1}.\text{year}^{-1})$ for the Ikkour watershed. In Erbil, north of Iraq, Keya [15] found that the soil loss rate was between 0.0 and 16.60 $(\text{ton.ha}^{-1}.\text{year}^{-1})$ for the Alibag watershed. In Mexico, López-García et al. [16] found that the average annual soil loss rate for Tzicatlacoyan, Puebla was 117.180 $(\text{ton.ha}^{-1}.\text{year}^{-1})$. In Jharkhand, India, Roy [17] found that the average annual soil erosion rate in the Irga watershed was 4.30 $(\text{ton.ha}^{-1}.\text{year}^{-1})$. In India, Ghosh et al. [18] found that the annual soil loss for the Mayurakshi river basin of eastern India was 4629714.8 (ton.year^{-1}). In Tunisia, Serbaji et al. [19] revealed that Tunisia has a serious risk of soil water erosion, and 6.43% of the total area of the country has a soil erosion rate of more than 30.00 $(\text{ton.ha}^{-1}.\text{year}^{-1})$, which is under the class of very high soil loss rate. In Manshera-Pakistan, Mehwish et al. [20] found that the annual soil loss for the Siran river basin was 0.154 million (ton) with an average rate of 0.871 $(\text{ton.ha}^{-1}.\text{year}^{-1})$.

2.TYPE OF SOIL EROSION

1- Splash Erosion (Raindrop Erosion): It is the initial water erosion that occurs when an erosive rainfall event occurs [21]. The splash erosion can displace the soil particles more than 5 m horizontally by wind [22] and 1.5 m high vertically [23].

2- Sheet Erosion: It is also called areal or laminar erosion and is considered a major threat to many developing countries [24]. A mixture of water and solid particles flows down the hillslope as a sheet, eroding the soil by consecutive layers [24].

3- Rill Erosion: It occurs due to the concentrated flow of water [25] and during heavy rainfall, when small rills form on the entire hillside, making the farming difficult [26]. Rills seem like small rivers that cut and bend through the soil [27]. The resulting rills may persist and develop into gullies, impeding more land use [28].

4- Gully Erosion: Due to its climate and lithology, gullies are particularly prevalent in the Mediterranean and tropical areas [24]. Some of the gullies formed are large, which will harm the farmers since they may be unable to cross them with farm machinery [26].

5- Stream Bank Erosion: It is considered a negative characteristic of rivers [29]. However, it is also an essential process

that may facilitate riparian vegetation succession and create dynamic habitats at different elevation zones that are important and necessary for aquatic and riparian animals and plants [30].

6- Wind Erosion: It is highly visible [26] and represents a dynamic and physical process in which bare, dry, and loose soils are transported due to intense winds [31].

3. SIGNIFICANT OF RESEARCH

The review of the available studies revealed only a few studies of soil erosion in the Kurdistan Region of Iraq (KRI). Due to the possibility that Harir Basin may be exposed to soil erosion and due to the importance of the study area as it is a significant residential, urban, agricultural, and tourist area. Therefore, this study was conducted to preserve the area and reduce soil erosion in the future by taking prior measures to confront this phenomenon and decrease its occurrence because soil erosion negatively affects water management, agricultural lands, and the region's environment.

4. OBJECTIVE OF THE STUDY

1- To estimate, create, and map the spatial distribution of the factors that affect the annual rate of soil erosion based on the (USLE), (RS), and (GIS) techniques in Harir Basin.

2- To investigate and illustrate the capability of (USLE), (RS), and (GIS) techniques in estimating the annual rate of soil erosion as well as creating and mapping the spatial distribution of the annual rate of soil erosion of Harir Basin and to classify the area of study according to the soil erosion risk classes.

5. NOVELTY OF WORK

Soil erosion is considered one of the most common hazards with significant consequences for rivers, reservoirs, soil, water quality, society, pollution, and the environment. The lack of vegetation cover, land topography, climate changes, environmental conditions, human activities, and the decrease in green spaces significantly increased the likelihood of soil erosion occurrences in the Kurdistan Region. It is critical to understand the causes, influencing variables, and geographic distribution of soil erosion as the factors that affect soil erosion, vulnerability, and risk to reduce and control this erosion. Due to a lack of studies in the Kurdistan Region of Iraq, this study investigates several fundamental aspects of soil erosion and soil erosion zonation, which will be significant for water, soil, and environment management.

6. THE STUDY AREA

The area of Harir Basin is 350.03 km², and in the north of Erbil governorate, the capital city of the Kurdistan Region of Iraq (KRI) between (36° 23' 00" N to 36° 39' 00" N) latitude and (44° 10' 00" E to 44° 29' 40" E) longitude, as illustrated in Fig. 1 (A). The study area consisted of fifty-nine villages, including Spilk, Batas, Harir, Basrma, and Flon, as demonstrated in Fig. 1 (B). The Digital Elevation Model (DEM) of Harir Basin with 30 m resolution was downloaded from the United States Geological Survey (USGS) website (https://earthexplorer.usgs.gov/) and re-projected to (WGS_1984_UTM_Zone_38N) by utilizing ArcGIS 10.8.1. The elevation of the basin according to the (DEM) ranges from 366 m to 1823 m, as shown in Fig. 1 (C), which is similar to the elevation found by [32] for this study area. Furthermore, several parts of the study area are illustrated in Fig. 1 (D), while the steps of creating and mapping the basin flowchart are demonstrated in Fig. 1 (E).

7. METHODOLOGY

7.1. Data Preparation

7.1.1. Flow Direction Map, Flow Accumulation Map, Drainage Network Map, Contour Map, Aspect Map, and Slope Classification Map in Percentage

For the present study, the flow direction map, flow accumulation map, drainage network map, contour map, aspect map, and slope map in percentage of Harir Basin have been created and mapped from the Digital Elevation Model (DEM) using ArcGIS 10.8.1. Moreover, the slope map was classified according to Table 1 [33].

Table 1 The Slope Classification in Percentage [33].

No.	Slope Classes	Slope in Percentage
1	Flat Area	0% to 3%
2	Undulating Slope	3% to 8%
3	Moderately Sloping	8% to 15%
4	Hilly	15% to 30%
5	Moderately Steep Slope	30% to 45%
6	Steep Slope	45% to 65%
7	Very Steep Slope	More than 65%

7.1.2. Average Annual Rainfall Map

In the present study, the average annual rainfall from (2000 to 2021) for five metrological stations (Harir, Khalifan, Shaqlawa, Rawanduz, and Soran) have been gathered from the Meteorological Department of the Ministry of Agriculture and Water Resources, Kurdistan Region Government (KRG)-Iraq in 2022 [34] to create and map the spatial distribution of the average annual rainfall for Harir Basin from (2000 to 2021) by utilizing the Inverse Distance Weighted (IDW) method in ArcGIS 10.8.1 software.

7.1.3. Soil Classification Map

For the present study, the shape file of the Digital Soil Map of the World (DSMW), which comes with attributes containing the percentages of silt, clay, sand, and organic carbon (OC), has been downloaded from the Food and Agriculture Organization (FAO) of the United Nations website [35]. Moreover, according to the area of study, the soil map for

the study area has been extracted and mapped from the (DSMW) by utilizing ArcGIS 10.8.1 and classified based on the data obtained from (FAO) and according to the soil texture triangle from the Natural Resources Conservation Service (NRCS), United States Department of Agriculture (USDA), as shown in Fig. 2 [36].
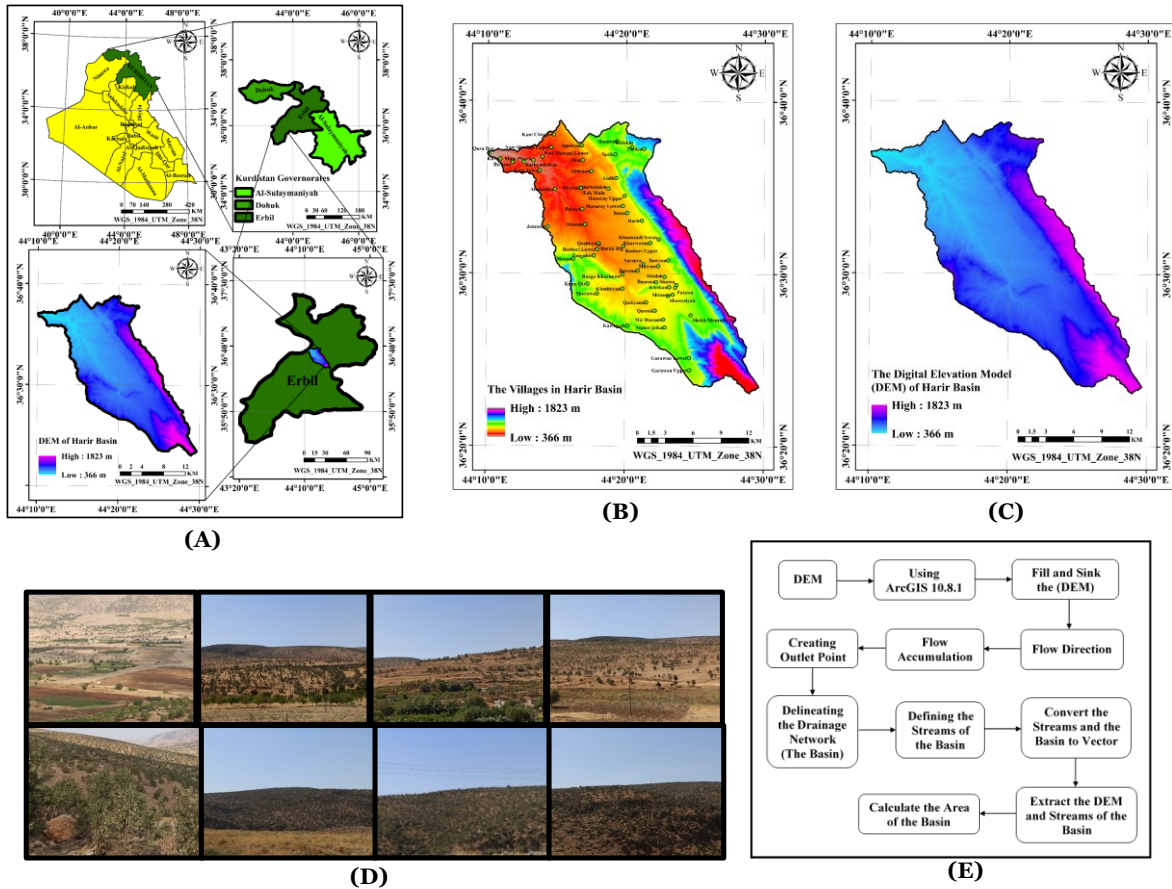
Fig. 1 (A) The Harir Basin Location. **(B)** The Villages in Harir Basin Location. **(C)** DEM of Harir Basin. **(D)** Several Parts of Harir Basin. **(E)** The Steps of Creating the Basin Flowchart.
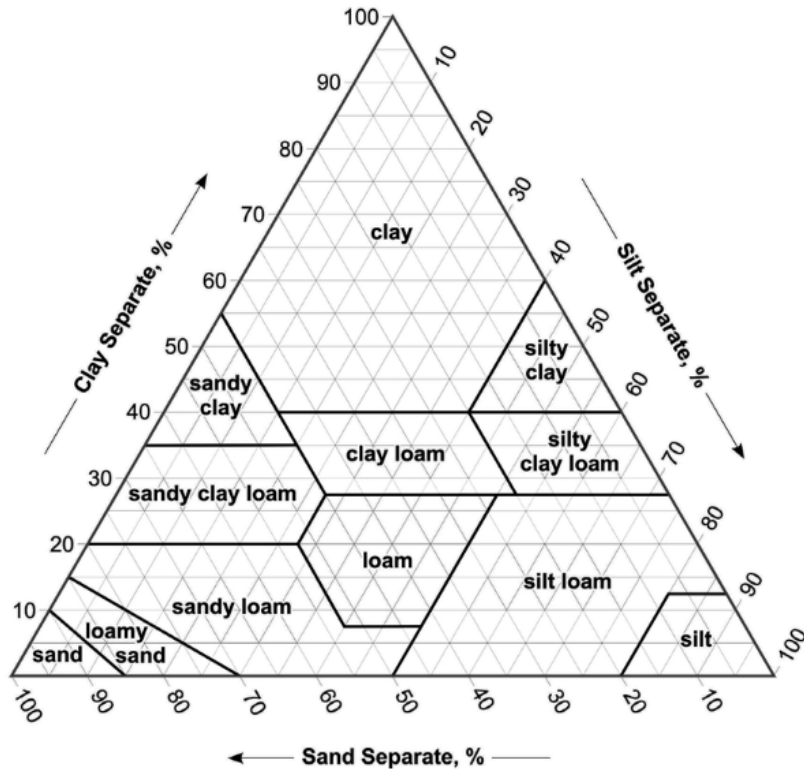
Fig. 2 Soil Texture Triangle.

7.1.4. Geological Formations Map

The geological formations map of Harir Basin was extracted and created from the geological map of (Erbil and Mahabat Quadrangles) using ArcGIS 10.8.1 to classify the geological formations of Harir Basin.

7.1.5. Normalized Difference Vegetation Index (NDVI) Classification Map

The Normalized Difference Vegetation Index (NDVI) ranges from -1 to 1 [37]. The high and low values of NDVI indicate that the lands have high and low vegetation cover, respectively [38]. For the present study, band 4 and band 5 of Landsat 9 Operational Land Imager (OLI) Images that were obtained on (13/April/2022) and downloaded from the (USGS) website have been combined by utilizing ArcGIS10.8.1, as shown in Fig. 3 (A), to calculate, create, and map the spatial distribution of the NDVI classes of Harir Basin and classify the basin based on Table 2 [39].

7.1.6. Land Use and Land Cover Classification Map and Accuracy Assessment

In the present study, the land use and land cover map was extracted and mapped from the Landsat 9 Operational Land Imager (OLI) Images with a 30 m spatial resolution for the study area obtained on (13/April/2022). The images were downloaded from the United States Geological Survey (USGS) website, i.e., (https://earthexplorer.usgs.gov/) and re-projected to (WGS_1984_UTM_Zone_38N) using ArcGIS 10.8.1. The seven bands, i.e., 1, 2, 3, 4, 5, 6, and 7, of multispectral images for the study area have been composited using ArcGIS 10.8.1. The Supervised Classification-Maximum Likelihood Classification (MLC) has been utilized to classify the land use and land cover for Harir Basin by utilizing the ERDAS Imagine 2014 software based on Landsat 9 OLI images. Then, it has been digitized (converted to vector) using ArcGIS 10.8.1. The properties of bands 1 to 7 of Landsat 9 OLI images according to (USGS) are shown in Table 3. The accuracy assessment is considered one of the most significant final steps in the classification process [40] and the essential factor used to evaluate the reliability of the map since there is no completed image classification unless its accuracy is evaluated [41]. For the present study, Eqs. (1-3) were used to calculate the overall accuracy, producer accuracy, and user accuracy, respectively [42], while Eq. (4) was used to calculate the Kappa coefficient for the land use and land cover classification of Harir Basin.

$$\text{Overall Accuracy} = \left(\frac{1}{N}\right) * \sum_{i=1}^{r} n_{ii} \qquad (1)$$

$$\text{Producer's Accuracy} = \left(\frac{n_{ii}}{n_{icol}}\right) \qquad (2)$$

$$\text{User's Accuracy} = \left(\frac{n_{ii}}{n_{irow}}\right) \qquad (3)$$

where N represents the total number of classified values versus truth values, r represents the number of rows, n_{ii} represents the number of appropriately categorized pixels in a category, and n_{icol} and n_{irow} are the column (reference data) and row (predicted classes) totals, respectively.

$$\text{Kappa Coefficient} = \frac{N \sum_{i=1}^{n} m_{i,i} - \sum_{i=1}^{n}(G_i C_i)}{N^2 - \sum_{i=1}^{n}(G_i C_i)} \qquad (4)$$

where N represents the total number of classified values versus truth values, n represents the number of rows/columns in the error matrix (confusion matrix), i represents the class number, $m_{i,i}$ represents the number of observations in column i and row i, C_i represents the total number of predicted values in class i, and G_i represents the total number of truth values in class i. The Kappa coefficient ranges between (0) and (1). When the Kappa coefficient is equal to (1) and (0), it indicates perfect agreement and no agreement, respectively [43]. Figure 3 (B) shows the flowchart of land use and land cover classification and the accuracy assessment process.

Table 2 The Normalized Difference Vegetation Index (NDVI) Classification [39].

No.	NDVI Classes	NDVI Ranges
1	Water	-0.28 - 0.015
2	Built-Up	0.015 - 0.14
3	Barren Land	0.14 - 0.18
4	Shrub and Grassland	0.18 - 0.27
5	Sparse Vegetation	0.27 - 0.36
6	Dense Vegetation	0.36 - 0.74

Table 3 The Properties of Bands 1 to 7 of Landsat 9 OLI Images According to (USGS).

No	Bands	Wavelength in (Micrometers)	Resolution in (Meters)
1	Band 1 - Coastal Aerosol	0.43-0.45	30
2	Band 2 - Blue	0.45-0.51	30
3	Band 3 - Green	0.53-0.59	30
4	Band 4 - Red	0.64-0.67	30
5	Band 5 - Near Infrared (NIR)	0.85-0.88	30
6	Band 6 - SWIR 1	1.57-1.65	30
7	Band 7 - SWIR 2	2.11-2.29	30

(A)

(B)
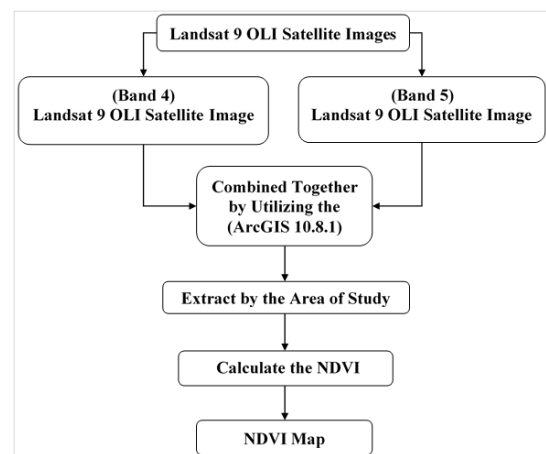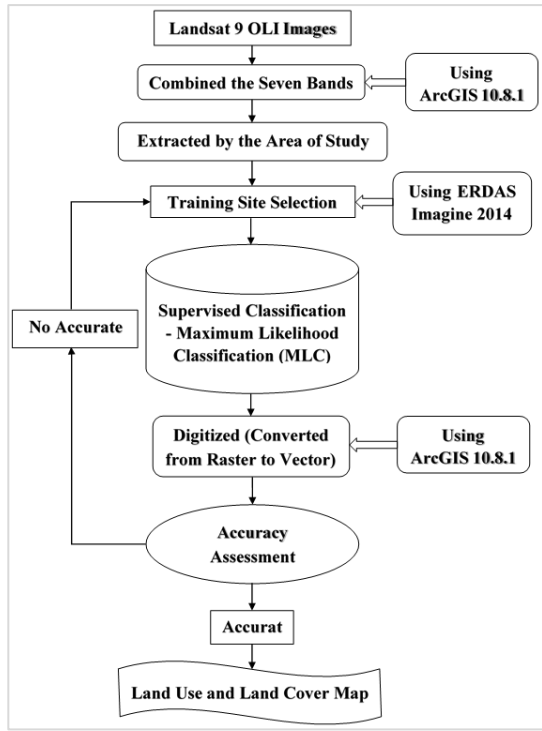
Fig. 3 (A) The Flowchart of the NDVI Classification, **(B)** The Flowchart of the Land Use and Land Cover Classification and the Accuracy Assessment Process of Harir Basin.

7.2. Universal Soil Loss Equation (USLE)

The Universal Soil Loss Equation (USLE) has been developed by the United States Agricultural Research Service. For the present study, the (USLE) has been applied to calculate the annual rate of soil erosion in Harir Basin based on Eq. (5) [44].

$$A = R * K * LS * C * P \qquad (5)$$

where (A), (R), (K), (LS), (C), and (P) represent the annual rate of soil erosion in $(ton. ha^{-1}. year^{-1})$, rainfall erosivity factor in $(MJ. mm. ha^{-1}. h^{-1}. year^{-1})$, soil erodibility factor in $(ton. ha. h. ha^{-1}. MJ^{-1}. mm^{-1})$, slope length and slope steepness factor (unitless), cropping management factor (unitless), and conservation practice factor (unitless), respectively. In the present study, the raster calculator from ArcToolbox in ArcGIS 10.8.1 has been utilized to apply the (USLE) by multiplying all the factors in raster format with each other to calculate, create, and map the spatial distribution of the annual rate of soil erosion of Harir Basin and classify the study area based on Table 4 [45].

Table 4 The Soil Erosion Classification [45].

No.	Soil Erosion Classes	Annual Rate of Soil Erosion in $(ton. ha^{-1}. year^{-1})$
1	Slight Erosion	0.0 – 5.0
2	Moderate Erosion	5.0 – 10.0
3	High Erosion	10.0 – 20.0
4	Very High Erosion	20.0 – 40.0
5	Severe Erosion	40.0 – 80.0
6	Very Severe Erosion	More than 80.0

7.2.1. Rainfall Erosivity Factor (R-Factor)

The rainfall erosivity factor (R-factor) can be defined as the soil erosion that was caused due to the aggressiveness of rainfall [46]. Furthermore, it demonstrates the detachment of soil particles from each other and the downslope transport of the soil particles due to soil cover, topography, amount of energy, and the rain intensity in similar soil [47]. For the present study, three methods (Equations) [48-50] were utilized to calculate the rainfall erosivity factor (R-factor) according to the climatological similarity and based on the average annual rainfall of Harir Basin from (2000 to 2021). Ferrari et al. [48] suggested Eq. (6) for Italy, Renard and Freimund [49] suggested Eq. (7) for Continental United States U.S., and Yu and Rosewell [50] suggested Eq. (8) for Southeastern Australia.

$$R = 4.0412P - 965.53 \qquad (6)$$
$$R = 0.0483P^{1.61} \qquad (7)$$
$$R = 0.0438P^{1.61} \qquad (8)$$

where (R) and (P) represent the rainfall erosivity factor (R-factor) in $(MJ. mm. ha^{-1}. h^{-1}. year^{-1})$ and the average annual rainfall in (mm), respectively. In the present study, the spatial distribution of the average rainfall erosivity factor (average (R-factor)) of Harir Basin has been created and mapped by utilizing the interpolation function (IDW) method in ArcGIS 10.8.1 software. Additionally, the area of study has been classified based on the average rainfall erosivity factor (average (R-factor)) and according to Table 5 [51].

Table 5 The Rainfall Erosivity Factor (R-Factor) Classification [51].

No.	Rainfall Erosivity Classes	Rainfall Erosivity in $(MJ. mm. ha^{-1}. h^{-1}. year^{-1})$
1	Low Rainfall Erosivity	R ≤ 2452
2	Medium Rainfall Erosivity	2452 < R ≤ 4095
3	Medium-Strong Rainfall Erosivity	4095 < R ≤ 7357
4	Strong Rainfall Erosivity	7357 < R ≤ 9810
5	Very Strong Rainfall Erosivity	R > 9810

7.2.2. Soil Erodibility Factor (K-Factor)

The soil erodibility factor (K-factor) is a measure that indicates the ability of soil particles to separate from each other and then transport from one place to other places due to several factors, including surface runoff and rainfall [52]. The K-factor depends on the chemical and physical properties of soils, such as the organic matter content, infiltration, shear strength, aggregate stability, and soil texture [53]. For the present study, according to [54], the K-factor for each type of soil texture was found based on the percentage of organic matter content (OMC%) and the soil textural class. Moreover, based on [55], the K-factor unit was converted into

$(ton. ha. h. ha^{-1}. MJ^{-1}. mm^{-1})$ for each soil type, as shown in Table 6. Furthermore, the percentage of (OMC) was calculated for each type of soil in the area of study by applying Eq. (9) [56]. The spatial distribution of the (K-factor) for the study area has been developed and mapped from the soil classification map of Harir Basin using ArcGIS 10.8.1 and based on the (OMC%) and according to Table 6.

$$OMC\% = 1.72 * OC\% \qquad (9)$$

where OC% represents the percentage of organic carbon.

Table 6 The Soil Erodibility Factor (K-Factor) Classification.

No.	Soil Textural Classes	Soil Erodibility Factor (K-Factor) in $(ton. ha. h. ha^{-1}. MJ^{-1}. mm^{-1})$		
		Average OMC	OMC< 2%	OMC> 2%
1	Clay	0.0288	0.0317	0.0276
2	Clay Loam	0.0394	0.0435	0.0370
3	Coarse Sandy Loam	0.0094	0.0094	0.0094
4	Fine Sand	0.0106	0.0118	0.0076
5	Fine Sandy Loam	0.0235	0.0288	0.0223
6	Heavy Clay	0.0223	0.0253	0.0200
7	Loam	0.0394	0.0447	0.0341
8	Loamy Fine Sand	0.0147	0.0200	0.0118
9	Loamy Sand	0.0053	0.0065	0.0053
10	Loamy Very Fine Sand	0.0511	0.0582	0.0329
11	Sand	0.0024	0.0041	0.0012
12	Sandy Clay Loam	0.0264	0.0264	0.0264
13	Sandy Loam	0.0170	0.0182	0.0159
14	Silt Loam	0.0499	0.0540	0.0488
15	Silty Clay	0.0341	0.0358	0.0341
16	Silty Clay Loam	0.0423	0.0464	0.0394
17	Very Fine Sand	0.0564	0.0605	0.0488
18	Very Fine Sandy Loam	0.0464	0.0540	0.0435

7.2.3. Slope Length and Slope Steepness Factor (LS-Factor)

The slope steepness factor (S-factor) and the slope length factor (L-factor) illustrate the effect of the slope gradient and the slope length on the rate of soil erosion, respectively [44]. In the present study, the spatial distribution of the slope length and slope steepness factor (LS-factor) for Harir Basin has been created and mapped by applying Eq. (10) [54] by utilizing the raster calculator from ArcToolbox in ArcGIS 10.8.1 and based on the slope map in percentage and flow accumulation map of the study area.

$$LS = (L/22.1)^m (0.065 + 0.0456 * S + 0.006541 * S^2) \qquad (10)$$

where (L) and (S) represent the slope length in (meter) calculated using Eq. (11) and the slope gradient in (percentage), respectively. While the value of (m) can be estimated based on the slope map in percentage and according to Table 7 [54].

$$L = Flow\ Accumulation\ Map * Raster\ DEM\ Cell\ Size \qquad (11)$$

Table 7 The Values of (m) [54].

No.	Slope in percentage	m
1	Slope < 1%	0.2
2	1%≤ Slope < 3%	0.3
3	3% ≤ Slope < 5%	0.4
4	Slope ≥ 5%	0.5

7.2.4. Cropping Management Factor (C-Factor)

The C-factor illustrates the direct and major effect of the management and cropping on the rate of soil erosion [57-59]. Moreover, it represents the soil loss ratio from a watershed or a region with a specific land cover and management to that from an identical area in tilled continuous fallow [44]. The C-factor range is between (0) and (1). When the value of the C-factor is close to zero (0) and equal to (1), it indicates a very strong land cover and no land cover, respectively [60]. For the present study, the spatial distribution of the C-factor for the study area has been developed and mapped from the land use and land cover classification map of Harir Basin using ArcGIS 10.8.1 and based on Table 8 [61-63].

Table 8 The Cropping Management Factor (C-Factor) Classification.

No.	Land Use and Land Cover Classes	C-Factor	References
1	Water	0	[63]
2	Bare Ground	1	[62]
3	Built Area	0.2	[63]
4	Scrub/Shrub	0.1	[61]
5	Crops	0.55	[62]
6	Trees	0.001	[63]

7.2.5. Conservation Practice Factor (P-Factor)

The conservation practice factor (P-factor) represents the effect of the farming system or the land use on the rate of soil erosion [60]. It is the soil loss ratio with a certain support practice, such as terracing, contouring, or strip cropping, to that with straight-row farming down and up the slope [44]. The P-factor range is between (0) and (1) based on managing the agricultural land. When the value of (P-factor) is close to (1) and (0), it indicates poor conservation practice and good conservation practice, respectively [14]. In the present study, the spatial distribution of the (P-factor) for Harir Basin has been created and mapped from the slope map of the study area in percentage by utilizing ArcGIS 10.8.1 and based on the farming methods according to Table 9 [64]. Figure 4 illustrates the overall flowchart of the methodology of soil erosion assessment.

Table 9 The Conservation Practice Factor (P-Factor) Classification [64].

No.	Slope in Percentage	Terracing	Strip Cropping	Contouring
1	0.0% - 7.0%	0.10	0.27	0.55
2	7.0% - 11.30%	0.12	0.30	0.60
3	11.30% - 17.60%	0.16	0.40	0.80
4	17.60% - 26.80%	0.18	0.45	0.90
5	>26.80%	0.20	0.50	1.00
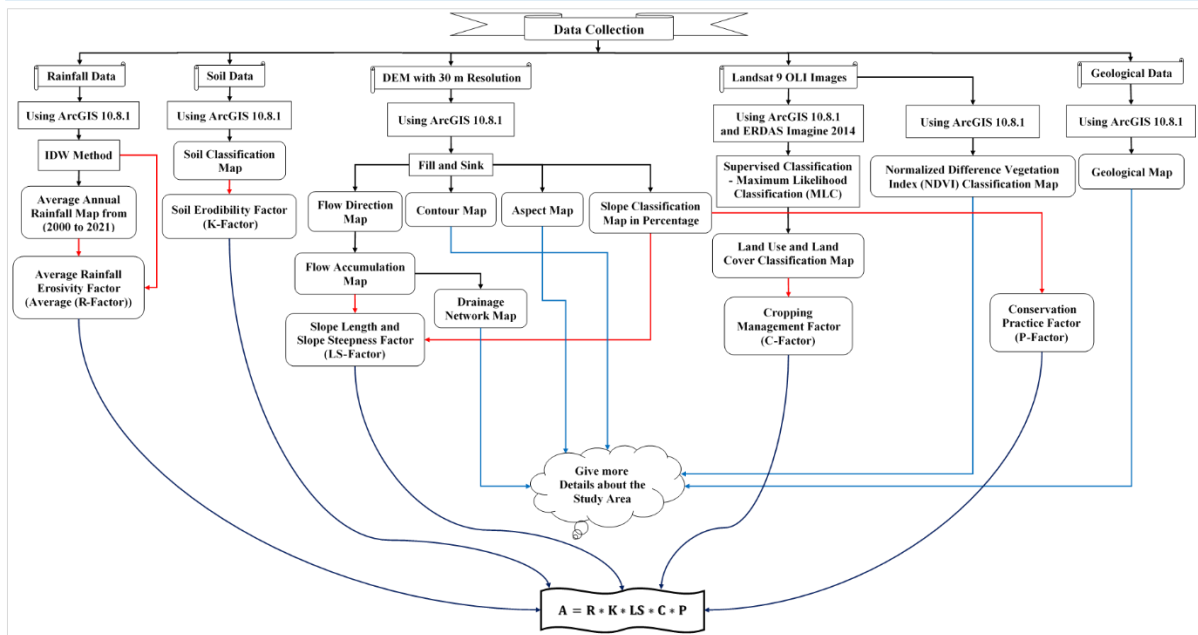
Fig. 4 The Methodology.

8. RESULTS AND DISCUSSION

8.1. Flow Direction Map, Flow Accumulation Map, Drainage Network Map, Contour Map, Aspect Map, and Slope Map in Percentage

Figures 5 (A-F) illustrate the spatial distribution of the flow direction map, flow accumulation map, drainage network map with the location of the outlet point and stream order, contour map, aspect map, and slope map in percentage (ranging from 0.0% to 228.8%) of Harir Basin, respectively. Table 10 shows the results of the slope classification map of Harir Basin.

8.2. Average Annual Rainfall Map, Soil Map, Geological Formations Map, Normalized Difference Vegetation Index (NDVI) Map, Land Use and Land Cover Map, and Accuracy Assessment

Figures 6 (A-E) show the spatial distribution of the average annual rainfall map from (2000 to 2021) (ranging from 619.013 mm to 774.173 mm) with the location of the metrological stations, which is similar to the results of average annual rainfall map found by [32] for this study area, soil map (where the classes are sandy clay loam soil and loam soil), geological formations map, normalized difference vegetation index (NDVI) map (where the classes are water, built-up, barren land, shrub and grassland, sparse vegetation, and dense vegetation), and land use and land cover map (where the classes are water (which is the portion of the Greater Zab (Upper Zab) River), bare ground, built area, scrub/shrub, crops, and trees) of Harir Basin, respectively. Tables 11-15 show the results of the average annual rainfall for each station, soil classification map, geological formations map, NDVI classification map, and land use and land cover classification map of Harir Basin, respectively. For the accuracy evaluation, 87 ground truth random points were created using ArcGIS 10.8.1 over the research region for the land use and land cover classification. The results revealed that the overall accuracy and Kappa coefficients of the generated land use and land cover layer were 95.4% and 93.2%, respectively, which is a perfect agreement according to [65]. Table 16 shows the error matrix of the accuracy assessment of land use and land cover classification map, while Table 17 illustrates the user accuracy% and the producer accuracy% of land use and land cover classes of Harir Basin.
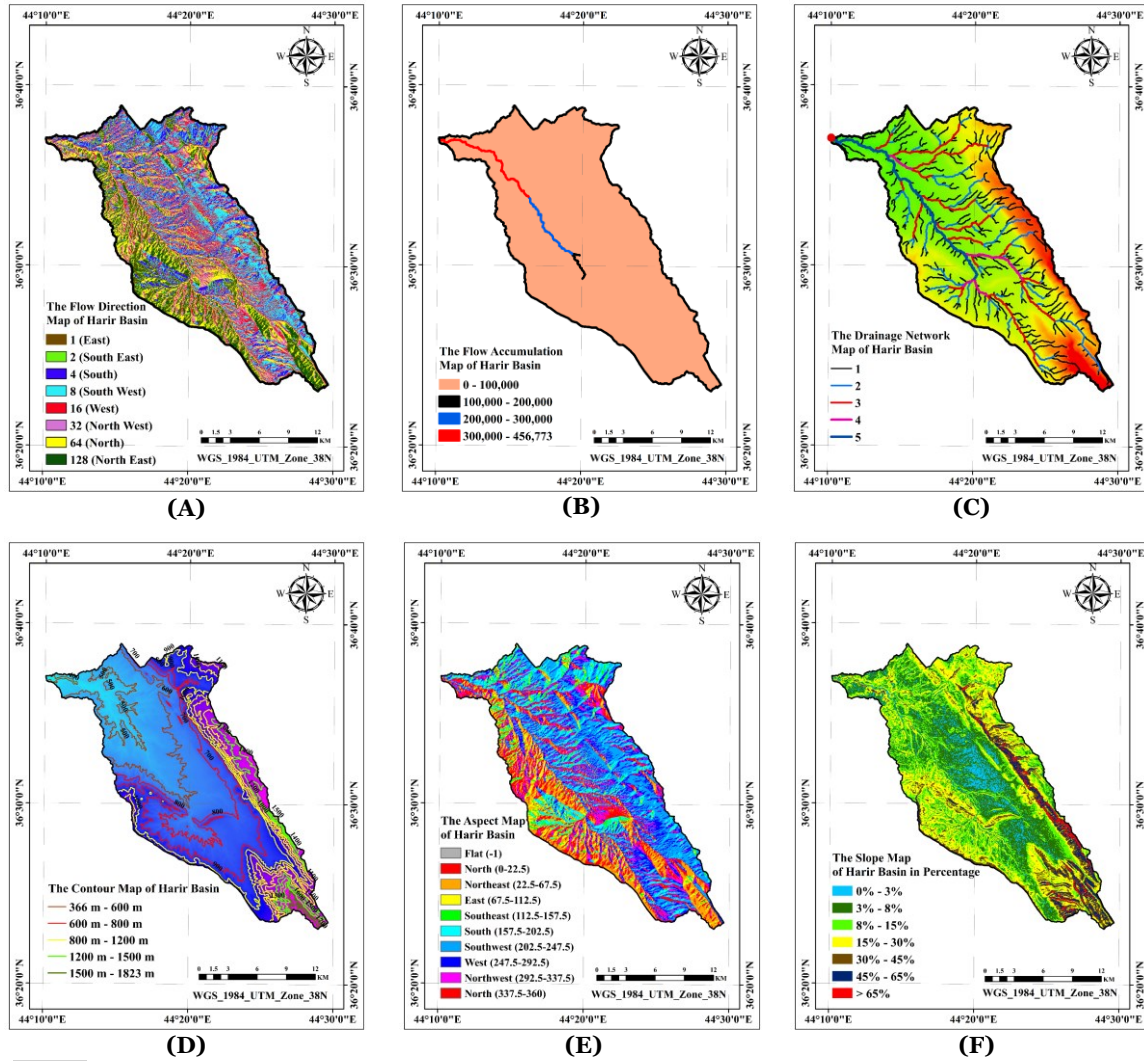
Fig. 5 The Spatial Distribution of the **(A)** Flow Direction Map. **(B)** Flow Accumulation Map. **(C)** Drainage Network Map with the Location of the Outlet Point and Stream Order. **(D)** Contour Map. **(E)** Aspect Map. **(F)** Slope Map in Percentage of Harir Basin.

Table 10 The Slope Classification of Harir Basin.

No.	Slope Classes	Slope in Percentage	Area %	Area in Km²
1	Flat Area	0% to 3%	7.93%	27.76
2	Undulating Slope	3% to 8%	27.24%	95.36
3	Moderately Sloping	8% to 15%	23.74%	83.11
4	Hilly	15% to 30%	25.57%	89.49
5	Moderately Steep Slope	30% to 45%	8.88%	31.07
6	Steep Slope	45% to 65%	4.89%	17.12
7	Very Steep Slope	More than 65%	1.75%	6.12

Table 11 The Average Annual Rainfall for Each Station.

No.	Stations	Latitude (N)	Longitude (E)	City	Average Annual Rainfall in (mm) from (2000 to 2021)
1	Harir	36.5514	44.3528	Erbil	619
2	Khalifan	36.6104	44.4064	Erbil	763
3	Soran	36.6518	44.5332	Erbil	697
4	Rawanduz	36.6081	44.5219	Erbil	732
5	Shaqlawa	36.3972	44.3366	Erbil	804

Table 12 The Soil Classification of Harir Basin.

No.	Percentage of Sand	Percentage of Silt	Percentage of Clay	Percentage of Organic Carbon	Type of Soil	Area %	Area in Km²
1	58.9%	16.2%	24.9%	0.97%	Sandy clay loam	86.13%	301.47
2	48.7%	29.7%	21.6%	0.64%	Loam	13.87%	48.56
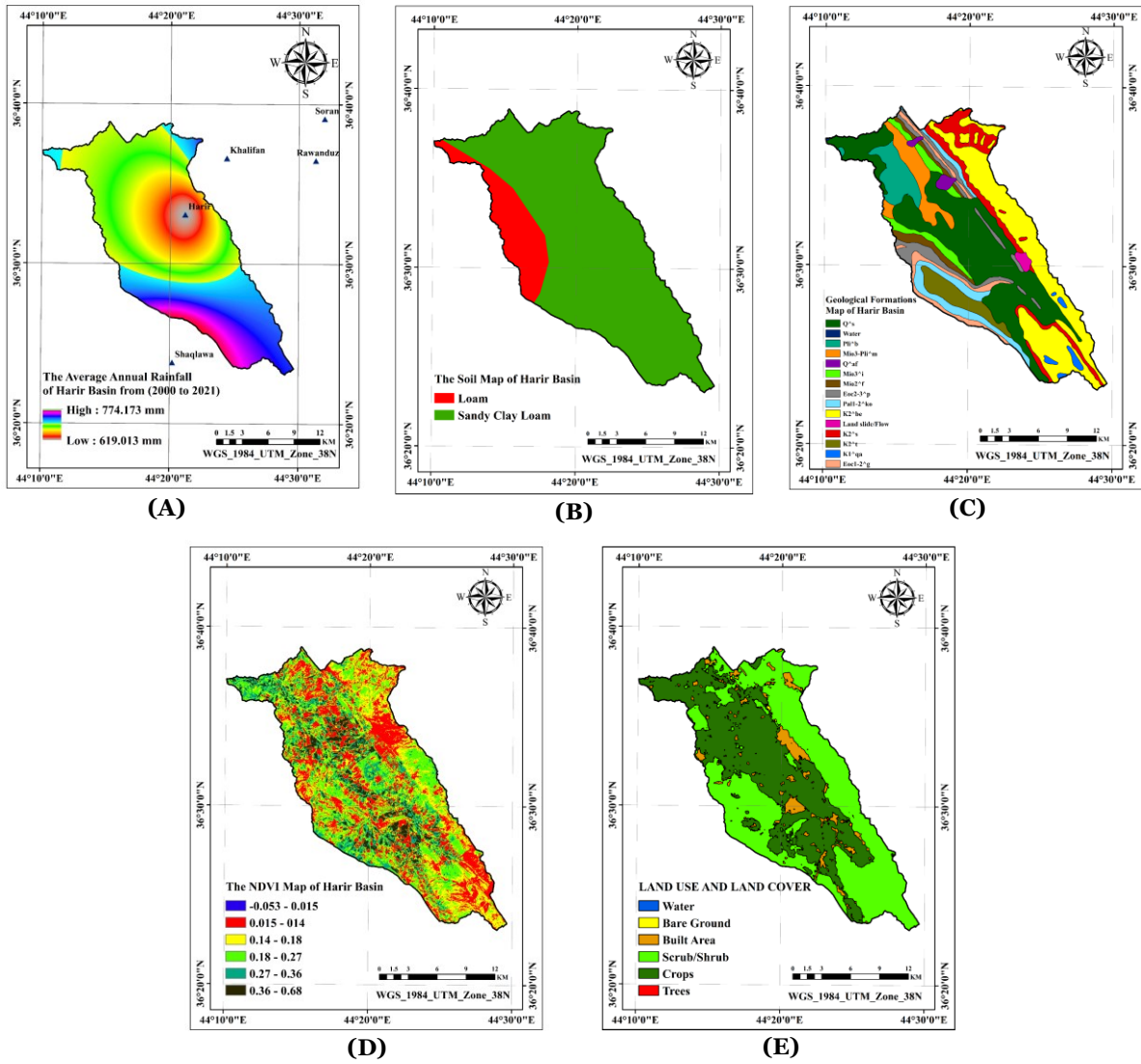
Fig. 6 The Spatial Distribution of the **(A)** Average Annual Rainfall Map from (2000 to 2021) with the Location of the Metrological Stations. **(B)** Soil Map. **(C)** Geological Formations Map. **(D)** Normalized Difference Vegetation Index (NDVI) Map. **(E)** Land Use and Land Cover Map of Harir Basin.

Table 13 The Geological Formations Classification of Harir Basin.

No.	Geological Classes	Description of Geological Classes	Formations of Geological Classes	Area%	Area in Km²
1	Q^S	Slope Deposits	Rock fragments with fine clastics	31.35%	109.745
2	Water	Water Area	water	0.03%	0.094
3	Pli^b	Bai Hassan (Upper Bakhtiari) Formation	Conglomerate, sandstone, and claystone	5.12%	17.905
4	$Mio_3 - Pli^m$	Mukdadiyah (Lower Bakhtiari) Formation	Pebbly sandstone, siltstone, and claystone	5.16%	18.077
5	Q^{af}	Alluvial Fan Deposits	Rock fragments, locally gravelly covered by a thin mantle of soil	0.9%	3.159
6	Mio_3^i	Injana (Upper Fars) Formation	Sandstone, siltstone, and claystone	3.46%	12.109
7	Mio_2^f	Fatha (Lower Fars) Formation	Gypsum, marl, limestone, red claystone, and siltstone	2.62%	9.154
8	Eoc_{2-3}^p	Pilaspi Formation	Includes mainly well-bedded limestones	5.22%	18.271
9	Pal_{1-2}^{ko}	Kolosh Formation	Black claystone, siltstone, and sandstone	5.56%	19.445
10	K_2^{be}	Aqra-Bekhme Formation (Locally with Kometan Formation)	Includes mainly well-bedded to massive limestones (Marly limestone)	23.09%	80.83
11	Land Slide/Flow	Land Slide/Flow	Land slide/flow	0.61%	2.136
12	K_2^s	Shiranish Formation	Well-bedded limestones and blue marl	8%	28.004
13	K_2^t	Tanjero Formation	Khaki sandstone and claystone, with conglomerate	4.21%	14.741
14	K_1^{qa}	Qamchuaqa Formation	Includes mainly massive limestones and dolomites	0.96%	3.369
15	Eoc_{1-2}^g	Gercus Formation	Red sandstone, siltstone, and claystone	3.71%	12.993

Table 14 The NDVI Classification of Harir Basin.

No.	NDVI Classes	NDVI Ranges	Area %	Area in Km²
1	Water	-0.053 - 0.015	0.01%	0.02
2	Built-Up	0.015 - 0.14	28.47%	99.65
3	Barren Land	0.14 - 0.18	23.02%	80.57
4	Shrub and Grassland	0.18 - 0.27	28.36%	99.26
5	Sparse Vegetation	0.27 - 0.36	12.69%	44.43
6	Dense Vegetation	0.36 - 0.68	7.45%	29.10

Table 15 The Land Use and Land Cover Classification of Harir Basin.

No.	Land Use and Land Cover Classes	Area%	Area in Km²
1	Water	0.01%	0.02
2	Bare Ground	0.47%	1.66
3	Built Area	5.73%	20.07
4	Scrub/Shrub	50.2%	175.69
5	Crops	43.57%	152.51
6	Trees	0.02%	0.08

Table 16 The Error Matrix of the Accuracy Assessment of Land Use and Land Cover Classification Map of Harir Basin.

Land Use and Land Cover Classes	Water	Bare Ground	Built Area	Scrub/Shrub	Crops	Trees	Total (User)
Water	1	0	0	0	0	0	1
Bare Ground	0	3	0	0	0	0	3
Built Area	0	0	18	0	0	0	18
Scrub/Shrub	0	0	0	37	4	0	41
Crops	0	0	0	0	23	0	23
Trees	0	0	0	0	0	1	1
Total (Producer)	1	3	18	37	27	1	87

Table 17 The User Accuracy% and the Producer Accuracy% of Land Use and Land Cover Classification Map of Harir Basin.

No.	Land Use and Land Cover Classes	User Accuracy%	Producer Accuracy%
1	Water	100%	100%
2	Bare Ground	100%	100%
3	Built Area	100%	100%
4	Scrub/Shrub	90.24%	100%
5	Crops	100%	85.19%
6	Trees	100%	100%

8.3. Annual Rate of Soil Erosion and the Factors According to the (USLE)

Figure 7 demonstrates the relation between the average rainfall erosivity factor (average (R-factor)) for each station and the average annual rainfall for each station. From this relation, Eq. (12) was obtained for this study, and it is represented as the average (R-factor) in the present study, which is a new equation that can also be used to calculate the rainfall erosivity factor for other catchment areas, basins, and watersheds in the Kurdistan Region of Iraq.

$$\textbf{Average (R-Factor)} = \textbf{4.0551} * \textbf{P} - \textbf{1043.9} \qquad \textbf{(12)}$$

where Average (R-Factor) and (P) represent the average rainfall erosivity factor in $(MJ.mm.ha^{-1}.h^{-1}.year^{-1})$ and the average annual rainfall in (mm), respectively. Table 18 shows the results of the average rainfall erosivity factor (average (R-factor)) for each station, while Figs. 8 (A-F) illustrate the spatial distribution of the average rainfall erosivity factor (Average (R-Factor)) (ranging from 1470.91 to 2100 $(MJ.mm.ha^{-1}.h^{-1}.year^{-1})$), soil erodibility factor (K-Factor), slope length and slope steepness factor (LS-Factor) (ranging from 0.0% to 293.43%, and the value of (m) is 0.5 in Eq. (10) because most of Harir Basin is under slope ≥ 5%), cropping management factor (C-Factor), conservation practice factor (P-Factor) (where the farming method for the study area is contouring), and the annual rate of soil erosion (ranging from 0.0 to 8.46 $(ton.ha^{-1}.year^{-1})$) of Harir Basin, respectively. Furthermore, Tables 19-24 illustrate the results of the average rainfall erosivity factor, soil erodibility factor, slope length and slope steepness factor, cropping management factor, conservation practice factor, and the annual rate of soil erosion of Harir Basin, respectively.
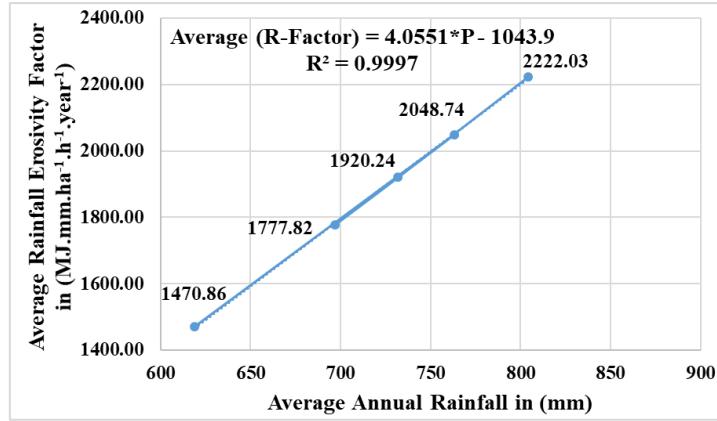
Fig. 7 The Relation Between the Average Rainfall Erosivity Factor for Each Station and the Average Annual Rainfall for Each Station.

Table 18 The Average Rainfall Erosivity Factor (Average (R-Factor)) for Each Station.

No.	Stations	Rainfall Erosivity Factor According to (Ferrari et al Method)	Rainfall Erosivity Factor According to (Renard & Freidmund Method)	Rainfall Erosivity Factor According to (Yu and Rosewell Method)	Average Rainfall Erosivity Factor in $(MJ.mm.ha^{-1}.h^{-1}.year^{-1})$
1	Harir	1535.97	1508.58	1368.03	1470.86
2	Khalifan	2117.91	2112.57	1915.75	2048.74
3	Soran	1851.19	1826.21	1656.07	1777.82
4	Rawanduz	1992.63	1976.10	1792.00	1920.24
5	Shaqlawa	2283.59	2298.31	2084.19	2222.03

(A)

(B)

(C)

(D)

(E)

(F)
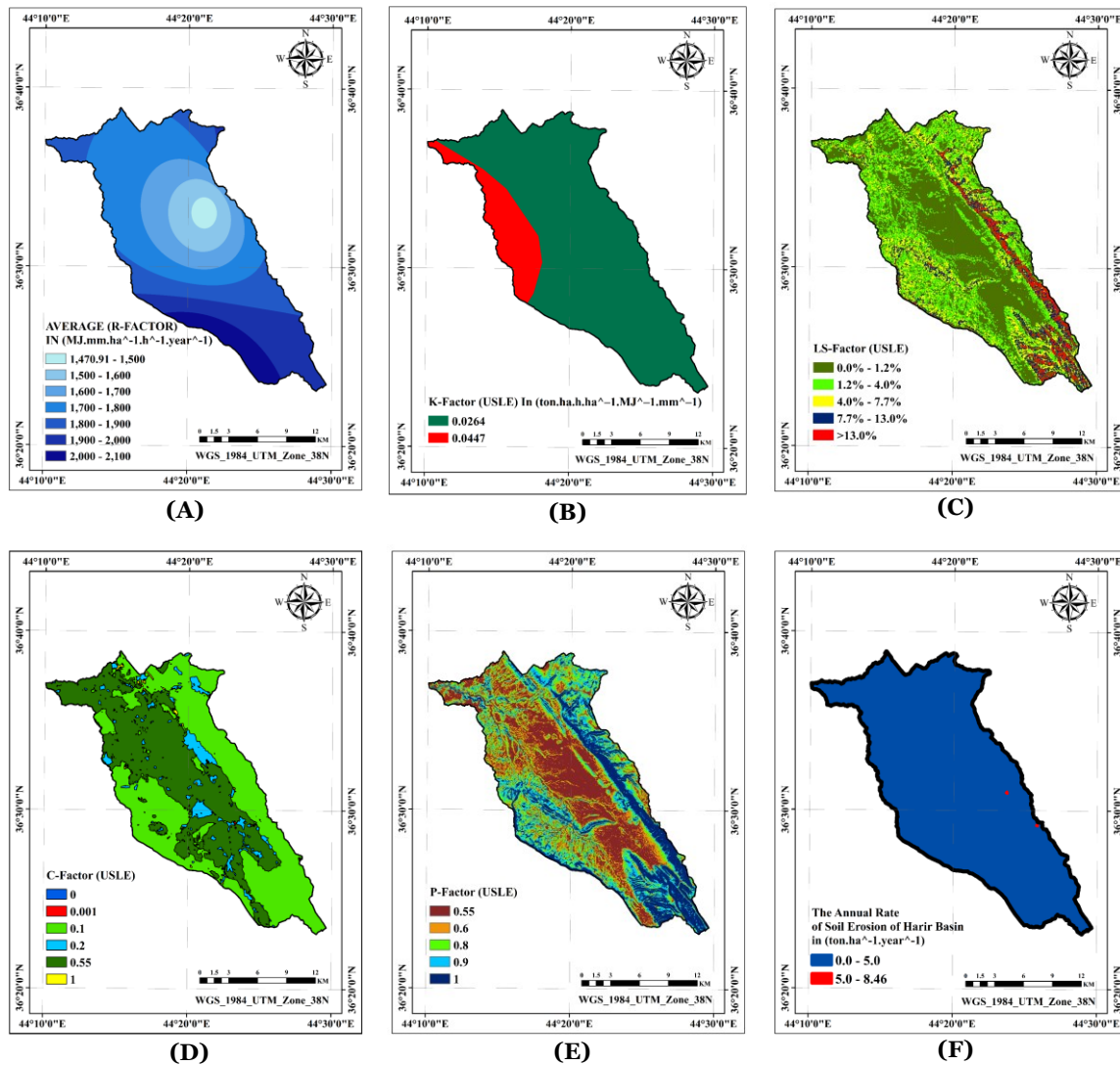
Fig. 8 The Spatial Distribution of the **(A)** Average (R-Factor) from (2000 to 2021), **(B)** (K-Factor), **(C)** (LS-Factor), **(D)** (C-Factor), **(E)** (P-Factor), **(F)** Annual Rate of Soil Erosion of Harir Basin.

Table 19 The Average Rainfall Erosivity Factor (Average (R-Factor)) Classification of Harir Basin.

No.	Average Rainfall Erosivity Factor in $(MJ.mm.ha^{-1}.h^{-1}.year^{-1})$	Rainfall Erosivity Classes	Area%	Area in Km^2
1	1470.91 to 1500	Low Rainfall Erosivity	1.94	6.78
2	1500 to 1600	Low Rainfall Erosivity	8.99	31.47
3	1600 to 1700	Low Rainfall Erosivity	15.33	53.67
4	1700 to 1800	Low Rainfall Erosivity	34.05	119.19
5	1800 to 1900	Low Rainfall Erosivity	16.62	58.16
6	1900 to 2000	Low Rainfall Erosivity	16.14	56.49
7	2000 to 2100	Low Rainfall Erosivity	6.93	24.27

Table 20 The Soil Erodibility Factor (K-Factor) Classification of Harir Basin.

No.	Type of Soil	Organic Carbon%	Organic Matter Content %	Soil Erodibility Factor (K-Factor) in $(ton.ha.h.ha^{-1}.MJ^{-1}.mm^{-1})$	Area %	Area in Km^2
1	Sandy Clay Loam	0.97%	1.67%	0.0264	86.13%	301.47
2	Loam	0.64%	1.1%	0.0447	13.87%	48.56

Table 21 The Slope Length and Slope Steepness Factor (LS-Factor) Classification of Harir Basin.

No.	LS-Factor	Area %	Area in Km^2
1	0% to 1.2%	88.72%	310.54
2	1.2% to 4.0%	6.99%	24.46
3	4.0% to 7.7%	2.24%	7.86
4	7.7% to 13.0%	0.98%	3.43
5	>13.0%	1.07%	3.74

Table 22 The Cropping Management Factor (C-Factor) Classification of Harir Basin.

No.	Land Use and Land Cover Classes	C-Factor	Area%	Area in Km^2
1	Water	0	0.01%	0.02
2	Bare Ground	1	0.47%	1.66
3	Built Area	0.2	5.73%	20.07
4	Scrub/Shrub	0.1	50.20%	175.69
5	Crops	0.55	43.57%	152.51
6	Trees	0.001	0.02%	0.08

Table 23 The Conservation Practice Factor (P-Factor) Classification of Harir Basin.

No.	Slope in percentage	Farming Method	P-Factor	Area%	Area in Km^2
1	0% to 7.0%	Contouring	0.55	31%	108.515
2	7.0% to 11.3%	Contouring	0.6	16.9%	59.215
3	11.3% to 17.6%	Contouring	0.8	17.5%	61.152
4	17.6% to 26.8%	Contouring	0.9	15.6%	54.701
5	More than 26.8%	Contouring	1	19%	66.447

Table 24 The Soil Erosion Classification of Harir Basin.

No.	Soil Erosion Classes	The Annual Rate of Soil Erosion in $(ton.ha^{-1}.year^{-1})$	Area%	Area in Km^2
1	Slight Soil Erosion	$0.0 - 5.0$	99.99%	350.00
2	Moderate Soil Erosion	$5.0 - 8.46$	0.01%	0.03

9.CONCLUSIONS

In the present study, the spatial distribution of the annual rate of soil erosion of Harir Basin has been created and mapped by utilizing the (USLE), (RS), and (GIS) techniques based on five factors, including the (Average (R-Factor)), (K-Factor), (LS-Factor), (C-Factor), and (P-Factor). The results of assessing Harir Basin against soil erosion showed that the (Average (R-Factor)) ranged from 1470.91 to 2100 $(MJ.mm.ha^{-1}.h^{-1}.year^{-1})$, and 100% of the study area was under the class of low rainfall erosivity. 86.13% and 13.87% of the study area had a (K-Factor) equal to 0.0264 and 0.0447 $(ton.ha.h.ha^{-1}.MJ^{-1}.mm^{-1})$, respectively. The (LS-Factor) ranged from (0.0% to 293.43%). 0.01%, 0.47%, 5.73%, 50.20%, 43.57%, and 0.02% of the study area had a (C-Factor) equal to 0, 1, 0.2, 0.1, 0.55, and 0.001, respectively. Moreover, 31%, 16.9%, 17.5%, 15.6%, and 19% of the study area had a (P-Factor) equal to 0.55, 0.6, 0.8, 0.9, and 1, respectively, and the farming method for the study area was contouring. The annual rate of soil erosion for

Harir Basin ranged from 0.0 $(ton.ha^{-1}.year^{-1})$ to 8.46 $(ton.ha^{-1}.year^{-1})$. 99.99% and 0.01% of the study area were under the slight and moderate soil erosion classes, respectively. Overall, assessing Harir Basin against soil erosion in Kurdistan Region-Iraq by using the (USLE), (RS), and (GIS) techniques has been conducted with the best accuracy, effectiveness, and efficiency.

10.RECOMMENDATIONS

1- Expand the present research to cover all the basins, watersheds, and catchment areas in the Kurdistan Region of Iraq (KRI).

2- Use other methods, such as Revised Universal Soil Loss Equation (RUSLE), Wind Erosion Equation (WEQ), Analytical Hierarchy Process (AHP), and Revised Wind Erosion Equation (RWEQ) and use other software tools, such as Soil and Water Assessment Tool (SWAT) and Quantum Geographic Information System (QGIS) to estimate, create, and map the spatial distribution of the annual

rate of soil erosion for other basins, watersheds, and catchment areas in the Kurdistan Region of Iraq (KRI).

3- Use the new equation of the average rainfall erosivity factor (average (R-factor)) obtained from the present research to estimate the rainfall erosivity factor (R-factor) for all Kurdistan Region of Iraq (KRI).

4- Install more meteorological stations in the Kurdistan Region of Iraq (KRI) and make better efforts to provide researchers with high-resolution remotely sensed data.

5- Identify the areas in the Kurdistan Region of Iraq (KRI) that may be subject to soil erosion in the future to provide advanced information on managing the basins, watersheds, and catchment areas and to find effective methods for managing water, soil, and the environment.

REFERENCES

[1] Angima S, Stott D, O'neill M, Ong C, Weesies G. **Soil Erosion Prediction Using Rusle for Central Kenyan Highland Conditions**. *Agriculture, Ecosystems & Environment* 2003; **97**(1-3):295–308.

[2] Pimentel D. **Soil Erosion: A Food and Environmental Threat**. *Environment, Development and Sustainability* 2006; **8**(1):119–137.

[3] Lal R. **Soil Degradation by Erosion**. *Land Degradation & Development* 2001; **12**(6):519–539.

[4] Sibbesen E. **Phosphorus, Nitrogen and Carbon in Particle-Size Fractions of Soils and Sediments**. *Surface Runoff, Erosion and Loss of Phosphorus at Two Agricultural Soils in Denmark, Plot Studies* 1989;1992:135–148.

[5] Steegen A, Govers G, Takken I, Nachtergaele J, Poesen J, Merckx R. **Factors Controlling Sediment and Phosphorus Export from Two Belgian Agricultural Catchments**. *Journal of Environmental Quality* 2001; **30**(4):1249–1258.

[6] Boardman J, Ligneau L, de Roo A, Vandaele K. **Flooding of Property by Runoff from Agricultural Land in Northwestern Europe**. *Geomorphology and Natural Hazards*: Elsevier; 1994. pp. 183–196.

[7] Verstraeten G, Poesen J. **The Nature of Small-Scale Flooding, Muddy Floods and Retention Pond Sedimentation in Central Belgium**. *Geomorphology* 1999; **29**(3-4):275–292.

[8] Meyer L, Bauer A, Heil R. **Experimental Approaches for Quantifying the Effect of Soil Erosion on Productivity**. *Soil Erosion and Crop Productivity* 1985:213–234.

[9] Oyedele J. **Effects of Erosion on the Productivity of Selected Southwestern Nigerian Soils**. Department of Soil Science, Obafemi Awolowo University, Ile-Ife, Nigeria; 1996.

[10] Valipour M. **Drainage, Waterlogging, and Salinity**. *Archives of Agronomy and Soil Science* 2014; **60**(12):1625–1640.

[11] Amore E, Modica C, Nearing MA, Santoro VC. **Scale Effect in USLE and Wepp Application for Soil Erosion Computation from Three Sicilian Basins**. *Journal of Hydrology* 2004; **293**(1-4):100–114.

[12] Sfeir-Younis A. **Soil Conservation in Developing Countries, Western Africa Projects Department**. The World Bank; 1986.

[13] Barrow CJ. **Land Degradation: Development and Breakdown of Terrestrial Environments**. Cambridge University Press; 1991.

[14] El Jazouli A, et al. **Soil Erosion Modeled with USLE, GIS, and Remote Sensing: A Case Study of Ikkour Watershed in Middle Atlas (Morocco)**. *Geoscience Letters* 2017; **4**(1):1–12.

[15] Keya D. **Integration of GIS with USLE in Assessing Soil Loss from Alibag Catchment, Iraqi Kurdistan Region**. *Journal of Polytechnic* 2018; **8**(1): 12-16.

[16] López-García EM, et al. **Estimation of Soil Erosion Using USLE and GIS in the Locality of Tzicatlacoyan, Puebla, México**. *Soil and Water Research* 2019; **15**(1):9–17.

[17] Roy P. **Application of USLE in a GIS Environment to Estimate Soil Erosion in the Irga Watershed, Jharkhand, India**. *Physical Geography* 2019; **40**(4):361–383.

[18] Ghosh A, Rakshit S, Tikle S, Das S, Chatterjee U, Pande CB, Mattar MA. **Integration of GIS and Remote Sensing with Rusle Model for Estimation of Soil Erosion**. *Land* 2022; **12**(1):116, (1-15).

[19] Serbaji MM, Bouaziz M, Weslati O. **Soil Water Erosion Modeling in Tunisia Using Rusle and GIS Integrated Approaches and Geospatial Data**. *Land* 2023; **12**(3):548, (1-22).

[20] Mehwish M, Nasir MJ, Raziq A, Al-Quraishi AMF, Ghaib FA. **Soil Erosion Vulnerability and Soil Loss Estimation for Siran River Watershed, Pakistan: An Integrated GIS and Remote Sensing Approach**.

Environmental Monitoring and Assessment 2024; **196**(1):104.

[21] Torres DS, Porrà JM, Creutin J-D. **A General Formulation for Raindrop Size Distribution**. *Journal of Applied Meteorology and Climatology* 1994; **33**(12):1494–1502.

[22] Erpul G, Gabriels D, Cornelis W, Samray H, Guzelordu T. **Sand Transport under Increased Lateral Jetting of Raindrops Induced by Wind**. *Geomorphology* 2009; **104**(3-4): 191–202.

[23] Ryżak M, Bieganowski A, Polakowski C. **Effect of Soil Moisture Content on the Splash Phenomenon Reproducibility**. *PLoS One* 2015; **10**(3):1–15.

[24] Descroix L, et al. **Gully and Sheet Erosion on Subtropical Mountain Slopes: Their Respective Roles and the Scale Effect**. *Catena* 2008; **72**(3):325–339.

[25] Knapen A, Poesen J, Govers G, Gyssels G, Nachtergaele J. **Resistance of Soils to Concentrated Flow Erosion: A Review**. *Earth-Science Reviews* 2007; **80**(1-2):75–109.

[26] Al-Kaisi M. **Soil Erosion: An Agricultural Production Challenge**. *Integrated Crop Management* 2000; **484**(19):141–143.

[27] Warren J. **Raindrops and Bombs: The Erosion Process**. Oklahoma Cooperative Extension Service; 2010.

[28] Guo M, Yang B, Wang W, Chen Z, Wang W, Zhao M, Kang H. **Distribution, Morphology and Influencing Factors of Rills under Extreme Rainfall Conditions in Main Land Uses on the Loess Plateau of China**. *Geomorphology* 2019; **345**: 106847, (1-15).

[29] Hughes A. **Riparian Management and Stream Bank Erosion in New Zealand**. *New Zealand Journal of Marine and Freshwater Research* 2016; **50**(2):277–290.

[30] Florsheim JL, Mount JF, Chin A. **Bank Erosion as a Desirable Attribute of Rivers**. *BioScience* 2008; **58**(6):519–529.

[31] Zobeck TM, Van Pelt RS. **Wind Erosion**. In: Hillel D, Hatfield J, Sauer T, Soil Management: Building a Stable Base for Agriculture. USA: American Society of Agronomy; 2011.

[32] Saber MJ, Suleimany JMS. **Application of Rs and GIS Techniques for Estimating the Rainfall Erosivity (R) of Harir River Basin in Kurdistan Region of Iraq Kri**. *Tikrit Journal of Engineering Sciences* 2022; **29**(3):24–32.

[33] Wahono BFD. **Applications of Statistical and Heuristic Methods for Landslide Susceptibility Assessments**. Unpublished Technical Report, Gadjah Mada University and International Institute for Geo-Information Science and Earth Observation; 2010.

[34] KRG. **Meteorological Department of the Ministry of Agriculture and Water Resources, Kurdistan Region Government (KRG), Iraq**. 2022.

[35] FAO. **Digital Soil Map of the World (DSMW) - Esri Shapefile Format**. Food and Agriculture Organization (FAO) of The United Nations; 2023. Available from: https://data.apps.fao.org/map/catalog/srv/eng/catalog.search#/metadata/446ed430-8383-11db-b9b2-000d939bc5d8

[36] Idowu J, Ghimire R, Flynn R, Ganguli A. **Soil Health: Importance, Assessment, and Management**. College of Agricultural, Consumer and Environmental Sciences; 2019.

[37] Usman U, Yelwa S, Gulumbe S, Danbaba A, Nir R. **Modelling Relationship between Ndvi and Climatic Variables Using Geographically Weighted Regression**. *Journal of Mathematical Sciences and Applications* 2013; **1**(2):24–28.

[38] Jasinski MF. **Sensitivity of the Normalized Difference Vegetation Index to Subpixel Canopy Cover, Soil Albedo, and Pixel Scale**. *Remote Sensing of Environment* 1990; **32**(2-3):169–187.

[39] Akbar TA, et al. **Investigative Spatial Distribution and Modelling of Existing and Future Urban Land Changes and Its Impact on Urbanization and Economy**. *Remote Sensing* 2019; **11**(2):105, (1-15).

[40] Rwanga SS, Ndambuki JM. **Accuracy Assessment of Land Use/Land Cover Classification Using Remote Sensing and GIS**. *International Journal of Geosciences* 2017; **8**(4): 611-622.

[41] Kaul HA, Sopan I. **Land Use Land Cover Classification and Change Detection Using High Resolution Temporal Satellite Data**. *Journal of Environment* 2012; **1**(4):146–152.

[42] Petropoulos GP, Kalivas DP, Georgopoulou IA, Srivastava PK. **Urban Vegetation Cover Extraction from Hyperspectral Imagery and Geographic Information System Spatial Analysis Techniques: Case of**

Athens, Greece. *Journal of Applied Remote Sensing* 2015; **9**(1):096088.

[43] Azen R, Walker CM. **Categorical Data Analysis for the Behavioral and Social Sciences**. Routledge; 2011.

[44] Wischmeier WH, Smith DD. **Predicting Rainfall Erosion Losses: A Guide to Conservation Planning**. U.S. Department of Agriculture, Agriculture Handbook No. 537; 1978.

[45] Singh G, Babu R, Narain P, Bhushan L, Abrol I. **Soil Erosion Rates in India**. *Journal of Soil and Water Conservation* 1992; **47**(1):97–99.

[46] Lal R. **Soil Erosion in the Tropics: Principles and Management**. McGraw-Hill; 1990.

[47] Ali SA, Hagos H. **Estimation of Soil Erosion Using USLE and GIS in Awassa Catchment, Rift Valley, Central Ethiopia**. *Geoderma Regional* 2016; **7**(2):159–166.

[48] Ferrari R, Pasqui M, Bottai L, Esposito S, Di Giuseppe E. **Assessment of Soil Erosion Estimate Based on a High Temporal Resolution Rainfall Dataset**. *7th European Conference on Applications of Meteorology (ECAM)*, Utrecht, Netherlands; 2005. pp. 12–16.

[49] Renard KG, Freimund JR. **Using Monthly Precipitation Data to Estimate the R-Factor in the Revised USLE**. *Journal of Hydrology* 1994; **157**(1-4):287–306.

[50] Yu B, Rosewell C. **Technical Notes: A Robust Estimator of the R-Factor for the Universal Soil Loss Equation**. *Transactions of the ASAE* 1996; **39**(2): 559–561.

[51] da Silva AM. **Rainfall Erosivity Map for Brazil**. *Catena* 2004; **57**(3):251–259.

[52] Erdogan EH, Erpul G, Bayramin İ. **Use of USLE/GIS Methodology for Predicting Soil Loss in a Semiarid Agricultural Watershed**. *Environmental Monitoring and Assessment* 2007; **131**(1):153–161.

[53] Hui L, Xiaoling C, Lim KJ, Xiaobin C, Sagong M. **Assessment of Soil Erosion and Sediment Yield in Liao Watershed, Jiangxi Province, China, Using USLE, GIS, and RS**. *Journal of Earth Science* 2010; **21**(6): 941–953.

[54] Stone R, Hilborn D. **Universal Soil Loss Equation (USLE) Factsheet**. Ontario Ministry of Agriculture, Food and Rural Affairs (OMAFRA); 2012.

[55] Foster G, McCool D, Renard K, Moldenhauer W. **Conversion of the Universal Soil Loss Equation to SI Metric Units**. *Journal of Soil and Water Conservation* 1981; **36**(6):355–359.

[56] De Lannoy GJ, Koster RD, Reichle RH, Mahanama SP, Liu Q. **An Updated Treatment of Soil Texture and Associated Hydraulic Properties in a Global Land Modeling System**. *Journal of Advances in Modeling Earth Systems* 2014; **6**(4):957–979.

[57] Biesemans J, Van Meirvenne M, Gabriels D. **Extending the Rusle with the Monte Carlo Error Propagation Technique to Predict Long-Term Average Off-Site Sediment Accumulation**. *Journal of Soil and Water Conservation* 2000; **55**(1):35–42.

[58] De Jong SM. **Derivation of Vegetative Variables from a Landsat Tm Image for Modelling Soil Erosion**. *Earth Surface Processes and Landforms* 1994; **19**(2):165–178.

[59] Patil R, Sharma S. **Remote Sensing and GIS Based Modeling of Crop/Cover Management Factor (C) of USLE in Shakker River Watershed**. *Proceedings of the International Conference on Chemical, Agricultural and Medical Sciences (CAMS-2013)*; 2013. pp. 29–30.

[60] Pham TG, Degener J, Kappas M. **Integrated Universal Soil Loss Equation (USLE) and Geographical Information System (GIS) for Soil Erosion Estimation in a Sap Basin: Central Vietnam**. *International Soil and Water Conservation Research* 2018; **6**(2):99–110.

[61] Bakker MM, et al. **The Response of Soil Erosion and Sediment Export to Land-Use Change in Four Areas of Europe: The Importance of Landscape Pattern**. *Geomorphology* 2008; **98**(3-4):213–226.

[62] Bouguerra H, Bouanani A, Khanchoul K, Derdous O, Tachi SE. **Mapping Erosion Prone Areas in the Bouhamdane Watershed (Algeria) Using the Revised Universal Soil Loss Equation through GIS**. *Journal of Water and Land Development* 2017; **32**: 13–23.

[63] Devatha C, Deshpande V, Renukaprasad M. **Estimation of Soil Loss Using USLE Model for Kulhan Watershed, Chattisgarh – A Case Study**. *Aquatic Procedia* 2015; **4**:1429–1436.

[64] Shin G. **The Analysis of Soil Erosion in Watershed Using GIS**. [PhD Thesis]. Department of Civil Engineering, Gangwon National University, Gangwon-do, South Korea; 1999.

[65] Cohen J. **A Coefficient of Agreement for Nominal Scales**. *Educational and Psychological Measurement* 1960; **20**(1): 37–46.